

## Structure–Activity Relationship Study of Prion Inhibition by 2-Aminopyridine-3,5-dicarbonitrile-Based Compounds: Parallel Synthesis, Bioactivity, and in Vitro Pharmacokinetics

Barnaby C. H. May,<sup>\*,†,‡</sup> Julie A. Zorn,<sup>§</sup> Juanita Witkop,<sup>†</sup> John Sherrill,<sup>§</sup> Andrew C. Wallace,<sup>§</sup> Giuseppe Legname,<sup>†,‡</sup> Stanley B. Prusiner,<sup>†,‡,#</sup> and Fred E. Cohen<sup>†,§</sup>

*Institute for Neurodegenerative Diseases and Departments of Neurology, Cellular and Molecular Pharmacology, and Biochemistry and Biophysics, University of California—San Francisco, San Francisco, California 94158*

Received August 31, 2006

2-Aminopyridine-3,5-dicarbonitrile compounds were previously identified as mimetics of dominant-negative prion protein mutants and inhibit prion replication in cultured cells. Here, we report findings from a comprehensive structure–activity relationship study of the 6-aminopyridine-3,5-dicarbonitrile scaffold. We identify compounds with significantly improved bioactivity (approximately 40-fold) against replication of the infectious prion isoform (PrP<sup>Sc</sup>) and suitable pharmacokinetic profiles to warrant evaluation in animal models of prion disease.

### Introduction

Misfolding of the cellular prion protein, PrP<sup>C</sup>, to a  $\beta$ -rich conformation, denoted PrP<sup>Sc</sup>, is the underlying molecular event that gives rise to the prion diseases.<sup>1</sup> Subsequent deposition of oligomeric PrP<sup>Sc</sup> in the central nervous system leads to neuronal loss and rapid death in animals and humans.<sup>2</sup> The conversion of PrP<sup>C</sup> to PrP<sup>Sc</sup> is thought to proceed via formation of a complex between the PrP isoforms and an as-yet unidentified molecular chaperone (Figure 1A, denoted "X").<sup>3</sup> The proposed PrP–X binding may involve an epitope that maps to dominant-negative PrP mutants, involving residues Q168 and Q172 of helix B and residues T215 and Q219 of helix C (Figure 1B, human PrP numbering).<sup>4</sup> Dominant-negative PrP mutants protect from disease, as demonstrated by familial polymorphisms in the human and ovine prion protein gene (*PRNP*),<sup>5,6</sup> transgenic animal models,<sup>7</sup> and transfection studies in scrapie-infected cells.<sup>4</sup>

In an effort to identify inhibitors to PrP<sup>Sc</sup> formation using a structure-based paradigm, computational chemistry was used to derive pharmacophore models based on the conformation and electronic space enciphered by dominant-negative mutant PrPs.<sup>8</sup> The pharmacophore models were used to query a virtual compound library to identify compounds that, given their mimicry of the dominant-negative epitope, might bind to the molecular chaperone "X". In binding the molecular chaperone, these ligands would occlude binding of PrPs and hence inhibit conversion of PrP<sup>C</sup>. Screening the candidate dominant-negative mimetic compounds in scrapie-infected neuroblastoma (ScN2a) cells identified a lead 2-aminopyridine-3,5-dicarbonitrile compound, **1** (Figure 1C).

As part of a structure–activity relationship (SAR) of this class of compound, we have identified 2-aminopyridine-3,5-dicarbonitrile compounds that are active at low micromolar concentrations in a scrapie-infected cell model of prion replication.

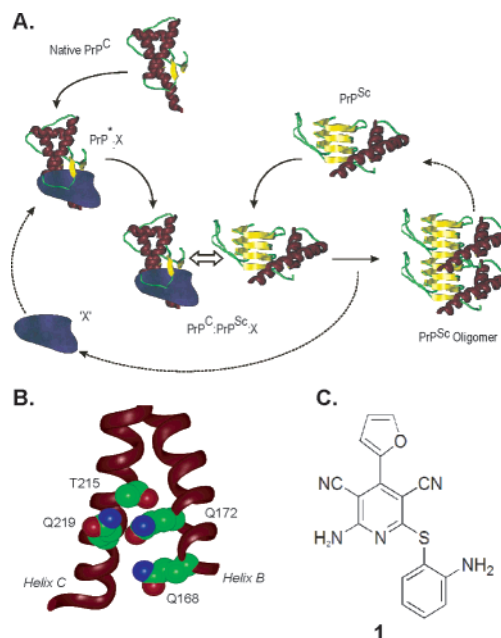


**Figure 1.** (A) Schematic diagram illustrating the conformational conversion of the cellular prion protein (PrP<sup>C</sup>) to the infectious isoform PrP<sup>Sc</sup>, which is thought to involve an unknown molecular chaperone, denoted "X". The representation of PrP<sup>Sc</sup> is based on the  $\beta$ -helical model of Govaerts et al.<sup>35</sup> (B) Dominant-negative epitope on the surface of PrP<sup>C</sup>, involving residues 168, 172, 215, and 219 (space-filled, based on numbering of the human PrP sequence). (C) Lead 2-aminopyridine-3,5-dicarbonitrile compound **1**.

Here, we present biological and in vitro pharmacokinetic data on a potent subset of 2-aminopyridine-3,5-dicarbonitrile compounds. These new lead compounds are characterized by a halobenzene and basic alkyl substituent at C-4 and C-6, respectively, of the pyridine heterocycle. Additionally, we identified a related potent scaffold, the thienopyridine. Certain newly identified analogues are approximately 40-fold more potent than the previous lead compounds in this class and possess suitable physicochemical properties for adsorption, distribution, metabolism, excretion, and toxicity (ADMET) and efficacy studies in animals.

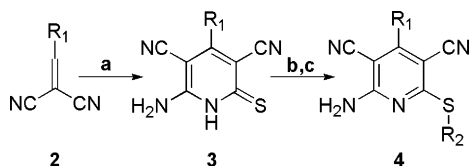
\* To whom correspondence should be addressed. Phone: 415-514-4243. Fax: 415-476-6515. E-mail: bmay@ind.ucsf.edu.

<sup>†</sup> Institute for Neurodegenerative Diseases.

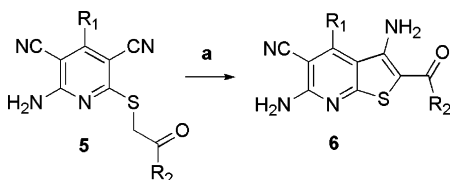
<sup>‡</sup> Department of Neurology.

<sup>§</sup> Department of Cellular and Molecular Pharmacology.

<sup>#</sup> Department of Biochemistry and Biophysics.

**Scheme 1<sup>a</sup>**

<sup>a</sup> Reagents and conditions: (a) 2-cyanothioacetamide (1 equiv), piperidine (1.5 equiv), EtOH, reflux, 8 h; (b) 10% KOH, DMF, room temp, 1 min; (c) aryl or alkyl halide, room temp, 5 h.

**Scheme 2<sup>a</sup>**

<sup>a</sup> Reagents and conditions: (a) 10% KOH, DMF, room temp, 5 h.

**Results**

**Library Synthesis.** The synthesis proceeded via formation of 2-(arylidene)malononitriles (**2**) via  $\beta$ -alanine catalyzed Knoevenagel condensation of malononitrile and commercially available aldehydes (Scheme 1).<sup>9</sup> Precursor 2-(arylidene)malononitriles (**2**) were isolated by filtration and used without further purification. The target pyridine compounds (**4**) were synthesized in a one-pot, two-step reaction, whereby 2-(arylidene)malononitriles (**2**) were first reacted with 2-cyanothioacetamide to yield the key intermediate (**3**).<sup>10</sup> Second, solvent was removed, and crude intermediates (**3**) were reacted with a chemset of alkyl halides and aryl halides in the presence of 10% aqueous KOH to furnish the C-6 substituent. The final products (**4**) were purified by parallel HPLC, and the library components were characterized by <sup>1</sup>H NMR and LCMS. In addition, a thienopyridine scaffold (Scheme 2, **6**) was also targeted to introduce rigidity to the C-6 substituent of the pyridine scaffold. Appropriately substituted pyridine compounds (**5**) were cyclized in the presence of 10% aqueous KOH to yield the corresponding substituted thienopyridines (**6**).<sup>10</sup> The original lead compound, **1**, was prepared as previously reported.<sup>11</sup> In total, 152 library components were synthesized.

**Duplex Cellular Screening Assay.** Scrapie-infected neuroblastoma cells (ScN2a)<sup>12</sup> were plated onto 96-well fluorescence compatible cell culture plates (approximately 40 000 cells/well) and incubated with compound for 5 days (approximately 150 000 cells/well). Compounds were initially screened at a single concentration point (20  $\mu$ M), and certain compounds were subsequently screened over a concentration range, up to 25  $\mu$ M. Following the viability assay, the calcein reagent was removed and intact ScN2a cells were treated with lysis buffer and Benzoylase to effect both cell lysis and concomitant poly-nucleic acid digestion. The cell lysates were then digested with proteinase K (PK) to yield the protease-resistant PrP fragment, PrP 27–30.<sup>13</sup> The digested lysates were treated with sodium phosphotungstic acid (PTA) and centrifuged to precipitate selectively PrP 27–30.<sup>14</sup> The pelleted fraction was denatured and coated onto Immulon II ELISA plates. PrP 27–30 was detected using the anti-PrP antibody D18<sup>15</sup> and goat anti-human IgG Fab alkaline phosphatase conjugate. Untreated ScN2a cells, no cells, and the antiprion compound quinacrine<sup>16</sup> were used as controls for the duplex assay. Dose-response curves over a concentration range were determined in triplicate from three independent experiments. Compound toxicity, as determined from the cell viability component of the assay, was expressed

as LD<sub>50</sub>, the compound concentration at which 50% of the cells were viable. Bioactivity against PrP<sup>Sc</sup> accumulation was expressed as EC<sub>50</sub>, the compound concentration at which 50% of PrP<sup>Sc</sup> had been removed from the culture on exposure to compound.

**Biological Activity.** Through iterative screening and synthesis we have identified 2-aminopyridine-3,5-dicarbonitrile compounds that are bioactive at low micromolar concentrations against PrP<sup>Sc</sup> accumulation and nontoxic up to 25  $\mu$ M. The placement of halobenzene substituents at C-4 of the scaffold provided improved activity to the 2-aminopyridine-3,5-dicarbonitrile compounds (Table 1, e.g., **7–14**). The meta-substituted monohalobenzene substituents were more potent than equivalent para-substituted analogues (Table 1; compare **7** and **8**). Particularly potent and nontoxic analogues were identified bearing basic alkyl substituents at C-6 of the pyridine heterocycle (Table 1, e.g., **17–23**). The bioactivity of such analogues was dependent on the size of the distal amine substituent (Table 1; compare **19** and **25**) and the length of the alkyl linker that separates the distal tertiary amine from the pyridine heterocycle (Table 1; compare **22** and **23**). While tertiary amines were bioactive at low micromolar concentrations, free amines and carboxamides (Table 1, **15** and **16**, respectively) were not effective even at concentrations up to 25  $\mu$ M. Rigidifying the C-6 substituent by cyclizing to a bicyclic thienopyridine heterocycle gave analogues that were bioactive at low micromolar concentrations (Table 1, **28** and **29**).

**In Vitro Pharmacokinetics.** A duplex solubility–permeability assay was adapted from the procedure of Wexler et al.<sup>17</sup> Compound solubility was categorized as follows: 0  $\mu$ M < “poor” < 200  $\mu$ M; 200  $\mu$ M < “medium” < 400  $\mu$ M; “excellent” > 400  $\mu$ M (Table 1). Membrane permeability was determined via a parallel artificial membrane permeability assay (PAMPA),<sup>18</sup> using a dioleoylphosphocholine (DOPC) lipid membrane, and log  $P_e$  was calculated using the equation of Wohlsland et al.<sup>19</sup> (Table 1). Estradiol, furosemide, chlorpromazine, guanabenz, methotrexate, carbamazepine, and famotidine were used as controls for the solubility and permeability assays and gave the expected relative pharmacokinetic profiles (Table 1).<sup>19</sup>

The duplex in vitro pharmacokinetic assay demonstrated that halobenzene-substituted analogues (Table 1, e.g., **11** and **12**), had limited solubility (<400  $\mu$ M). However, the relatively high PAMPA permeability rates for compounds in this series suggested that suitable serum concentrations may still be attainable. Compounds substituted with tertiary amines at C-6 of the pyridine scaffold demonstrated the potential to partition effectively into serum based on their solubility–permeability results. Compounds **18**, **19**, **22**, and **23** had solubilities in aqueous buffer greater than 400  $\mu$ M and PAMPA permeability rates equivalent to or better than those of the controls (Table 1). Thienopyridine compounds **28** and **29** had low solubility and readily precipitated in aqueous buffer and thus require further medicinal chemistry to optimize the physicochemical properties of this class.

**Modeling Studies.** The dominant-negative epitope on the surface of PrP involving residues Q168, Q172, T215, and Q219 was modeled and represented as a pharmacophore model as described previously (Figure 2A).<sup>8</sup> Multiple conformers of compounds **1** and **12** and the novel thienopyridine **28** were generated with the programs CORINA,<sup>20</sup> followed by OMEGA,<sup>21</sup> using the MMFF94 force field, a maximum of 400 conformations with a minimum distance of 0.6 Å between conformations, and an energy window of 20. The program GENX<sup>8</sup> was used to match the molecular conformers with the PrP pharmacophore

**Table 1.** Bioactivity and in Vitro Pharmacokinetic Properties of 2-Aminopyridine-3,5-dicarbonitrile Compounds

Cpd <sup>a</sup>	4, R <sub>1</sub>	4, R <sub>2</sub>	EC <sub>50</sub> ± SE <sup>b</sup> (μM)	LD <sub>50</sub> ± SE <sup>c</sup> (μM)	Solubility <sup>d</sup>	LogP <sub>c</sub> ± SE <sup>e</sup>	Cpd <sup>a</sup>	4, R <sub>1</sub>	4, R <sub>2</sub>	EC <sub>50</sub> ± SE <sup>b</sup> (μM)	LD <sub>50</sub> ± SE <sup>c</sup> (μM)	Solubility <sup>d</sup>	LogP <sub>c</sub> ± SE <sup>e</sup>
1			≈80-100	>80	low	ND	19			8.8 ± 0.9	>25	high	-6.0 ± 0.0
7			7.5 ± 1.0	>25	medium	-6.2 ± 0.1	20			13.4 ± 1.3	>25	ND	ND
8			5.3 ± 1.4	>25	low	-6.2 ± 0.0	21			10.6 ± 1.2	>25	medium	-6.2 ± 0.1
9			5.5 ± 2.0	>25	high	-6.0 ± 0.1	22			8.1 ± 0.7	>25	high	-6.0 ± 0.1
10			6.1 ± 1.0	>25	medium	-6.3 ± 0.0	23			6.0 ± 0.6	>25	high	-6.0 ± 0.1
11			4.3 ± 0.7	>25	low	-6.3 ± 0.1	24			NA	>25	ND	ND
12			2.2 ± 1.0	>25	low	-6.4 ± 0.1	25			NA	>25	ND	ND
13			4.5 ± 1.9	>25	medium	-6.2 ± 0.1	26			NA	>25	ND	ND
14			7.2 ± 1.5	>25	medium	-6.4 ± 0.2	27			NA	>25	ND	ND
15			NA <sup>f</sup>	>25	ND	ND	28			10.9 ± 2.8	>25	low	ND
16			NA	>25	ND	ND	29			18.5 ± 2.9	>25	low	ND
17			13.9 ± 1.2	>25	ND	ND	Quinacrine		0.8 ± 0.1	7.8 ± 0.1	high	-6.6 ± 0.2	
18			10.2 ± 2.8	>25	high	-6.5 ± 0.1	Estradiol		ND	ND	low	ND	
							Furosemide		ND	ND	high	-7.5 ± 0.5	
							Chlorpromazine		ND	ND	high	-6.3 ± 0.1	
							Quanabenz		ND	ND	low	-6.0 ± 0.7	
							Methotrexate		ND	ND	high	-8.0 ± 0.2	

<sup>a</sup> A complete list of 2-aminopyridine-3,5-dicarbonitrile compounds synthesized and for which full dose-response curves were obtained is available as Supporting Information online. <sup>b</sup> Compound concentration required to reduce PrP<sup>Sc</sup> to 50% relative to untreated control ScN2a cells. <sup>c</sup> Compound concentration required to reduce the number of viable cells to 50% relative to untreated control ScN2a cells. <sup>d</sup> Compound solubility at 500 μM in aqueous 50 mM potassium phosphate (monobasic), pH 6.5 buffer. Compound solubility was classified as follows: 0 μM < “poor” < 200 μM; 200 μM < “medium” < 400 μM; “excellent” > 400 μM. <sup>e</sup> PAMPA permeability across a DOPC lipid membrane. <sup>f</sup> NA, no activity up to 25 μM. ND, not determined. Standard error determined from three independent experiments.

model; a rms distance of less than 2 Å was classified as a match. The resulting matched molecular conformers were visualized with MOE<sup>22</sup> to determine which conformers best satisfied the electronic and steric constraints of the PrP pharmacophore model (Figure 2B–D).

## Discussion

Deriving a SAR for 2-aminopyridine-3,5-dicarbonitrile compounds required the development of a screening assay that would provide the necessary throughput and high-quality data needed to identify trends over the compound library. Existing approaches to quantify compound bioactivity against cellular PrP<sup>Sc</sup> suffer from poor quantitation and/or an absence of a microtiter plate format.<sup>16,23,24</sup> We envisaged a duplex microtitre plate-based screening assay that would quantify both compound toxicity

and cellular PrP<sup>Sc</sup>, using the same compound-treated cell culture. Quantification of toxicity was beneficial. First, toxic compounds gave false positives in the quantification of PrP<sup>Sc</sup>, and second, toxicity data were helpful in selecting nontoxic compounds for further study. Previously, we have shown that compound toxicity toward ScN2a cells correlates well with toxicity toward human kidney HEK92 and liver HEPG2 cells.<sup>25</sup> The duplex screening assay developed as part of this current work quantified cell viability using the fluorescent probe calcein-AM<sup>26</sup> and subsequently quantified PrP 27–30 by direct ELISA. Quantification of compound toxicity and efficacy against PrP<sup>Sc</sup> using the duplex assay gave Z factors of 0.7–0.8 and 0.5–0.6, respectively, and thus provided the necessary dynamic range and low deviation for screening purposes.<sup>27</sup> The ability to quantify both compound toxicity and efficacy from the same cell culture and the

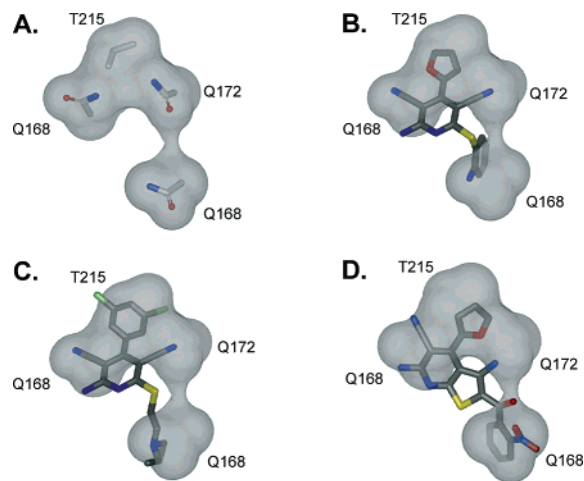


**Figure 2.** (A) Dominant-negative epitope on the surface of PrP<sup>C</sup>, involving residues 168, 172, 215, and 219. Also shown are the overlay of the dominant-negative epitope (gray) and (B) the original 2-aminopyridine-3,5-dicarbonitrile lead **1**, (C) compound **12**, and (D) thienopyridine compound **28**.

amenability to high-throughput screening are two unique benefits of the current duplex screening assay.

The original lead compound **1** (Table 1) was screened in the duplex assay and was weakly bioactive, EC<sub>50</sub> ≈ 80–100 μM. The discrepancy between our findings and those originally published for compound **1** (EC<sub>50</sub> = 20 μM)<sup>8</sup> can be attributed to the alternative cellular assays used to quantify bioactivity. Whereas the current duplex assay quantifies changes in total accumulated PrP<sup>Sc</sup>, the previous screening assay quantified changes in newly formed PrP<sup>Sc</sup>. Screening against newly formed PrP<sup>Sc</sup> requires transient transfection of ScN2a cells, typically with a mouse–hamster chimeric (MHM2) PrP.<sup>8</sup> In this way, newly formed PrP<sup>Sc</sup> can be distinguished from pre-existing PrP<sup>Sc</sup> using antibodies directed against the hamster sequence of the chimera. We chose to forego this approach, as transient transfection of ScN2a cells suffers from variable efficiency and reduces the overall robustness of the cellular screening assay.

Chemistries were identified and optimized that allowed for the parallel solution synthesis of the 2-aminopyridine-3,5-dicarbonitrile scaffold with diverse substituents at C-4 and C-6 of the pyridine heterocycle. In the first instance, aldehyde, aryl halide, and alkyl halide chemsets were selected in such a way that the resultant compound library encoded diverse chemical space with C-4 and C-6 substituents. We did not computationally filter target library components with the original pharmacophore used to identify the 2-aminopyridine-3,5-dicarbonitrile scaffold. Instead, traditional SAR was used to guide the focus of subsequent smaller compound libraries such that promising bioactive structural motifs at C-4 and C-6 could be explored in greater detail. Generally, a variety of substituents were tolerated at both the C-4 and C-6 positions of the pyridine heterocycle (see Supporting Information). Compound **10**, bearing a 4-bromobenzene substituent at C-4, and compound **19**, bearing a *N,N*-diethylamine substituent at C-6, were identified as promising leads from a larger diverse compound library. The SAR of compounds **10** and **19** was further elaborated with smaller focused compound libraries (Table 1) and identified compounds active at low micromolar concentrations. Compounds in these series would be candidates for subsequent medicinal chemistry optimizations. Cyclization of certain pyridine compounds yielded a novel class of bioactive thienopyridine compounds (Scheme 2). In some instances, certain thienopyridine com-

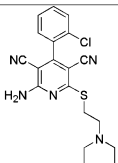
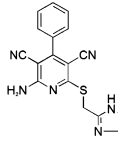
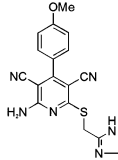
pounds (**6**) were more potent than the corresponding pyridine compounds (**5**) (see Supporting Information). The improved bioactivity of the thienopyridine scaffold may be attributed to the additional rigidity provided by the bicyclic scaffold that went some way toward preorganizing the C-6 substituent into a relevant receptor-bound conformation.

To complement compound toxicity and efficacy data and to improve the criteria by which bioactive 2-aminopyridine-3,5-dicarbonitrile compounds are selected for detailed *in vivo* studies, we implemented secondary assays for compound solubility and membrane permeability. These pharmacokinetic parameters are important determinants of the effective free-serum concentration of a compound following oral administration.<sup>28</sup> In developing *in vitro* pharmacokinetic screens, we did not aim to predict accurately partitioning of test compounds but rather to guide the selection of candidate compounds for further *in vivo* studies by providing relevant pharmacokinetic properties. Ideally, a compound would have an *in vitro* aqueous solubility greater than 400 μM and permeability constant greater than −7.0, as determined by the duplex solubility–permeability assay. Several new 2-aminopyridine-3,5-dicarbonitrile leads satisfied these criteria (Table 1), and subsequent *in vivo* pharmacokinetic studies are planned to validate the pharmacokinetic profiles of these compounds.

Identifying relevant cellular targets for the 2-aminopyridine-3,5-dicarbonitrile compounds would obviously aid the development of this class as therapeutics for the treatment of prion disease. Additionally, target identification and mechanistic insights would be important to understanding the cellular replication of PrP<sup>Sc</sup>. The original lead 2-aminopyridine-3,5-dicarbonitrile compound **1** was identified computationally as a dominant-negative PrP mimetic. However, it remains to be established whether compound **1** and related bioactive compounds in the class inhibit prion replication in ScN2a cells by binding to an unknown replication auxiliary “X” (Figure 1). A retrospective study was used to determine if 2-aminopyridine-3,5-dicarbonitrile compounds identified in the current work still satisfied the original pharmacophore used to identify dominant-negative mimetics. Computational modeling studies confirmed that newly identified 2-aminopyridine-3,5-dicarbonitrile compound **12** and the thienopyridine compound **28** spatially mimic the dominant-negative epitope encoded on the surface of PrP (Figure 2). However, additional studies are required to validate experimentally the binding of certain 2-aminopyridine-3,5-dicarbonitrile compounds to a macromolecule that participates in prion replication and hence validate the proposed mechanism of action of this class.

The possibility exists that alternative mechanisms may be responsible for the observed bioactivity of 2-aminopyridine-3,5-dicarbonitrile compounds in a cellular context. Reddy et al. have proposed that certain 2-aminopyridine-3,5-dicarbonitrile compounds bind PrP<sup>C</sup> to exert their effect in scrapie-infected cells.<sup>29</sup> Reddy et al. docked a virtual library of 2-aminopyridine-3,5-dicarbonitrile compounds against a putative binding pocket on the surface of PrP<sup>C</sup> and demonstrated that several hits interacted weakly with PrP<sup>C</sup>. However, the lead 2-aminopyridine-3,5-dicarbonitrile compounds from that study were generally inactive in scrapie-infected cells.<sup>29</sup> In comparison, we have used bioactivity in ScN2a cells to optimize our lead 2-aminopyridine-3,5-dicarbonitrile compounds for activity against PrP<sup>Sc</sup>. None of the lead 2-aminopyridine-3,5-dicarbonitrile compounds described by Reddy et al. overlap with those of our own work. To compare the relative bioactivity of known PrP<sup>C</sup>-binding 2-aminopyridine-3,5-dicarbonitrile compounds with our

**Table 2.** Bioactivity of 2-Aminopyridine-3,5-dicarbonitrile Compound **9** against Human Adenosine Receptor Subtypes hA<sub>1</sub>, hA<sub>2a</sub>, and hA<sub>3</sub>

Cpd	hA <sub>1</sub>	hA <sub>2a</sub>	hA <sub>3</sub>	ScN2a EC <sub>50</sub> ±SE (μM) <sup>b</sup>
 <b>9</b>	95% <sup>a</sup> <i>K</i> <sub>i</sub> =590 nM <sup>c</sup>	62% <sup>a</sup>	77% <sup>a</sup>	5.5±2.0 μM
 <b>30</b>	ND	ND	ND	>25
 <b>31</b>	ND	ND	ND	>25
DPCPX	ND	<i>K</i> <sub>i</sub> =3 nM <sup>c</sup>	ND	>25
NECA	ND	ND	<i>K</i> <sub>i</sub> =680 nM <sup>c</sup>	ND
IB-MECA	ND	ND	<i>K</i> <sub>i</sub> =2 nM <sup>c</sup>	>25

<sup>a</sup> Inhibition of human adenosine receptor subtypes hA<sub>1</sub>, hA<sub>2a</sub>, and hA<sub>3</sub> at a ligand concentration of 5 μM, relative to the known selective inhibitors also assayed at 5 μM: DPCPX (8-cyclopentyl-1,3-dipropylxanthine, 100% inhibition hA<sub>1</sub>), NECA (adenosine-5'-*N*-ethylcarboxamide, 100% inhibition hA<sub>2a</sub>), or IB-MECA (*N*-6-(3-iodobenzyl)adenosine-5'-*N*-methyluronamide, 100% inhibition hA<sub>3</sub>). <sup>b</sup> Bioactivity in ScN2a cells. Standard error determined from three independent experiments. <sup>c</sup> Inhibitor dissociation constant. ND, not determined.

own lead compounds, we independently synthesized the sole bioactive 2-aminopyridine-3,5-dicarbonitrile compound identified by Reddy et al., **27**. We determined that compound **27** was inactive up to 25 μM in our duplex ScN2a cell assay. These results suggest that while certain 2-aminopyridine-3,5-dicarbonitrile compounds may interact weakly with PrP<sup>C</sup> via a suitable binding pocket, alternative mechanisms leading to potentially more potent inhibition of PrP<sup>Sc</sup> replication may be operating in cellular models of prion replication.

Previously, compounds bearing the 2-aminopyridine-3,5-dicarbonitrile scaffold have been shown to be potent antagonists of adenosine receptors.<sup>30,31</sup> For example, compounds **30** and **31** (Table 2) bind human adenosine receptor subtypes with inhibitory constants in the nanomolar concentration range (for **30**, *K*<sub>i</sub>(hA<sub>1</sub>) = 2.4 ± 1.0 nM, *K*<sub>i</sub>(hA<sub>2a</sub>) = 28 ± 4 nM, *K*<sub>i</sub>(hA<sub>3</sub>) = 171 ± 109 nM; for **31**, *K*<sub>i</sub>(hA<sub>1</sub>) = 7.0 ± 0.8 nM, *K*<sub>i</sub>(hA<sub>2a</sub>) = 214 ± 37 nM, *K*<sub>i</sub>(hA<sub>3</sub>) = 24 ± 7.6 nM).<sup>30</sup> To investigate whether 2-aminopyridine-3,5-dicarbonitrile compounds elicit their antiprion effects in ScN2a cells via adenosine receptors, we determined whether the representative compound **9** was an adenosine receptor antagonist. Compound **9** was active at 5 μM against human hA<sub>1</sub>, hA<sub>2a</sub>, and hA<sub>3</sub> receptors and had an inhibitory constant of *K*<sub>i</sub> = 590 nM against hA<sub>1</sub> (Table 2). However, compound **9** was approximately 100- to 300-fold less potent against the adenosine receptor subtypes than the two known 2-aminopyridine-3,5-dicarbonitrile compounds **30** and **31** (Table 2).<sup>30</sup> Additionally, we synthesized compounds **30** and **31** and assayed these 2-aminopyridine-3,5-dicarbonitrile compounds, along with the structurally unrelated and potent adenosine antagonists 8-cyclopentyl-1,3-dipropylxanthine (DPCPX)<sup>32</sup> and *N*-6-(3-iodobenzyl)-adenosine-5'-*N*-methyluronamide (IB-MECA),<sup>33</sup> in ScN2a cells. These potent adenosine receptor

antagonists were inactive in ScN2a cells at 25 μM. It is noted that human and mouse adenosine receptors share significant sequence homology in the ligand-binding epitopes. These results suggest that the antiprion activity of 2-aminopyridine-3,5-dicarbonitrile compounds may not be attributed to adenosine receptor binding. Additional studies are needed to elucidate the mechanism of action of this class, potentially via suitably functionalized chemical genetics probes based on the 2-aminopyridine-3,5-dicarbonitrile scaffold.

## Conclusion

In conclusion, potent 2-aminopyridine-3,5-dicarbonitrile compounds have been identified that inhibit accumulation of PrP<sup>Sc</sup> in a cell model of prion replication at low micromolar concentrations. Current lead compounds in this series represent a marked improvement in bioactivity over the original lead compound. A detailed SAR for bioactive 2-aminopyridine-3,5-dicarbonitrile compounds has been defined, which includes a tertiary alkylamine of limited steric bulk at position C-6 and a mono- or dihalobenzene substituent at position C-4 of the pyridine scaffold. A novel bicyclic thienopyridine scaffold was identified as being effective against prion replication in culture. A qualitative assessment of lead compounds from this series has identified candidate compounds for further in vivo pharmacokinetic and efficacy evaluation in animal models of prion disease. Additionally, these current leads are of suitable potency to form the basis of chemical genetics probes with which to identify targets that may be implicated in prion replication.

## Experimental Section

**Chemistry and Biology. General Methods.** Malononitrile, β-alanine, and 2-cyanothioacetamide were purchased from Sigma-Aldrich Chemical Co. All aldehydes, aryl halides, and alkyl halides were purchased from either Sigma-Aldrich Chemical Co. or Maybridge Chemical Co. All solvents were obtained commercially in the highest purity (Sigma-Aldrich Chemical Co.) and used without further purification. Compound libraries were synthesized in parallel using a Bohdan 48-well, temperature-controlled miniblock fitted with a water-cooled condenser. Solvent was removed from individual reaction vessels using a Genevac HT-4 speedvac. Crude reactions were purified using a Parallelex Flex (Biotage) parallel preparative HPLC instrument fitted with Xterra C-18 columns (Waters) and automated fraction collector. Solvent was removed from fractions using a custom-built Genevac megaevaporator. <sup>1</sup>H and <sup>13</sup>C NMR data were recorded on a Varian 400 MHz spectrometer in either DMSO-*d*<sub>6</sub> or CD<sub>3</sub>OD/acetic acid-*d*<sub>4</sub>. LCMS was conducted on a Waters Micromass ZQ in ESI<sup>+</sup> mode, equipped with a Waters 2487 dual wavelength absorbance detector and Waters Alliance 2695 separations module, with the sample eluting through an analytical Xterra C-18 column. Compound purity was determined by LCMS using either method A (Waters Xterra C-18 column (2.1 mm × 50 mm, 3.5 μm) eluting water (0.05% trifluoroacetic acid)/methanol (0.05% trifluoroacetic acid), flow rate 0.2 mLmin<sup>-1</sup>, run time of 30 min) or method B (Waters Xterra phenyl column (2.1 mm × 50 mm, 3.5 μm) eluting water (0.05% trifluoroacetic acid)/acetonitrile (0.05% trifluoroacetic acid), flow rate 0.3 mLmin<sup>-1</sup>, run time of 20 min). Purity was determined from integrating peak areas of the liquid chromatogram, monitored at 254 nm. High-resolution mass spectrometry (HRMS) data were obtained by the Vincent Coates Foundation Mass Spectrometry Laboratory, Stanford University Mass Spectrometry. Compound structures, associated spectral data, and biological activity were stored as a chemical database using ISIS/Base (MDL, San Ramon). Sodium phosphotungstic acid (PTA), guanidine thiocyanate, diethanolamine, phenylmethylsulfonyl fluoride (PMSF), *p*-nitrophenyl phosphate tablets, and bovine serum albumin (BSA) were obtained from Sigma-Aldrich Chemical Co. Minimal essential media (MEM) with Earles salts, phosphate-buffered saline (PBS) without Ca<sup>2+</sup>

and  $Mg^{2+}$ , trypsin-EDTA, and GlutaMax were purchased from Gibco. Fetal bovine sera (FBS) were obtained from HyClone, and PK was from Invitrogen. Benzoylase nuclease was obtained from Novagen. Anti-PrP Fab antibody D18 was prepared in-house, and goat antihuman IgG Fab alkaline phosphatase conjugate was purchased from Fisher Scientific. Fluorescence intensity was determined using a Tecan Genios fluorescence microplate reader running XFluor4 software. Absorbance was determined using a SpectraMax Plus microplate reader running SoftMaxPro. ELISA plates were washed and aspirated using a Bio-Tek Elx405 plate washer. Plate-to-plate transfers and liquid dispensing were done using a Labctye S4 liquid handler fitted with a fixed 96-well head. Adenosine receptor binding studies were conducted by Cerep (Poitiers, France) using established methods.<sup>34</sup>

**General Procedure A. Synthesis of 2-Aminopyridine-3,5-dicarbonitrile Compounds.** Starting 2-(arylidene)malononitriles (**2**) were prepared from commercially available arylaldehydes using the procedure of Gazit et al. Briefly, a solution of the arylaldehyde (1 mmol), malononitrile (3 mmol), and a catalytic amount of  $\beta$ -alanine (approximately 0.4 mmol) in ethanol (30 mL) was stirred at room temperature for 72 h. The mixture was cooled on ice, and  $H_2O$  was added (10 mL) to precipitate the product. In cases for which the product remained soluble, solvent volume was reduced to half under vacuum, and the product precipitated on cooling. The product was removed by filtration, washed with ice-cold  $H_2O$  (5 mL), ice-cold ethanol (5 mL), and hexanes (5 mL) and dried under high vacuum. 2-(Arylidene)malononitriles were obtained in 60–95% yields, with purity of >90% as determined by LCMS, and were used without further purification.

To each well of a Bohdan miniblock, 2-(arylidene)malononitrile (**2**, 0.5 mmol), piperidine (0.75 mmol), and 2-cyanothioacetamide (0.5 mmol) in ethanol (3 mL) were added. The mixture was heated at 80 °C for 5 h with stirring. Solvent and piperidine were removed under vacuum centrifugation to yield the crude thione intermediates (**3**). The crude intermediates were resuspended in DMF (0.2 mL) and stirred with 10% KOH (1 equiv, 0.28 mL) at room temperature for 1 min. Aryl or alkyl halides (0.5 mmol) were added, and the mixture was stirred at room temperature for 5 h. Reaction vessels were again transferred to a Genevac HT4 speedvac, and solvent was removed. The crude products were resuspended in DMSO and purified using a Parallax Flex (Biotage) parallel preparative HPLC instrument fitted with Xterra C-18 columns (Waters). A solvent gradient of 10–100% methanol/20 mM ammonium acetate and a flow rate of 20 mL  $min^{-1}$  were employed. Injections were monitored using a UV absorbance at 254 nm, and fractions were collected using an automated fraction collector. Solvent was removed from all fractions using a Genevac megaevaporator. Aliquots of each fraction were analyzed by LCMS to determine purity and compound identity. Fractions were combined on this basis and solvent removed under reduced pressure to yield the target compounds as solids. All final compounds were characterized by  $^1H$  NMR and LCMS. Yields for the library ranged from approximately 10% to 70%. Compounds were dissolved in DMSO at a stock concentration of 10 mM and stored at –20 °C.

**2-Amino-4-(4-chlorophenyl)-6-(2-(diethylamino)ethylthio)pyridine-3,5-dicarbonitrile (7).**  $^1H$  NMR ( $CD_3OD/CD_3CO_2D$ )  $\delta$  7.57 (d,  $J = 8.4$  Hz, 2H), 7.51 (d,  $J = 8.8$  Hz, 2H), 3.60 (m, 2H), 3.48 (m, 2H), 3.34 (q,  $J = 7.2$  Hz, 4H), 1.35 (t,  $J = 7.2$  Hz, 6H); LCMS (ESI)  $m/z$  386 ( $MH^+$ ); HRMS  $m/z$  calculated for  $C_{19}H_{21}N_5ClS$  ( $MH^+$ ) 386.1206, found 386.1202; purity method A, 98%, method B, 95%.

**2-Amino-4-(3-chlorophenyl)-6-(2-(diethylamino)ethylthio)pyridine-3,5-dicarbonitrile (8).**  $^1H$  NMR ( $CD_3OD/CD_3CO_2D$ )  $\delta$  7.58 (d,  $J = 6.4$  Hz, 1H), 7.55 (m, 2H), 7.44 (dd,  $J = 1.6, 7.2$  Hz, 1H), 3.60 (m, 2H), 3.48 (m, 2H), 3.34 (q,  $J = 7.2$  Hz, 4H), 1.35 (t,  $J = 7.2$  Hz, 6H); LCMS (ESI)  $m/z$  386 ( $MH^+$ ); HRMS  $m/z$  calculated for  $C_{19}H_{21}N_5ClS$  ( $MH^+$ ) 386.1206, found 386.1199; purity method A, 93%, method B, 100%.

**2-Amino-4-(2-chlorophenyl)-6-(2-(diethylamino)ethylthio)pyridine-3,5-dicarbonitrile (9).**  $^1H$  NMR ( $CD_3OD/CD_3CO_2D$ )  $\delta$  7.62 (dd,  $J = 1.2, 8.0$  Hz, 1H), 7.56 (td,  $J = 1.6, 8.0$  Hz, 1H), 7.50 (td,

$J = 1.2, 7.2$  Hz, 1H), 7.39 (dd,  $J = 1.6, 7.6$  Hz, 1H), 3.60 (m, 2H), 3.48 (m, 2H), 3.34 (q,  $J = 7.2$  Hz, 4H), 1.35 (t,  $J = 7.2$  Hz, 6H); LCMS (ESI)  $m/z$  386 ( $MH^+$ ); HRMS  $m/z$  calculated for  $C_{19}H_{21}N_5ClS$  ( $MH^+$ ) 386.1206, found 386.1209; purity method A, 95%, method B, 95%.

**2-Amino-4-(4-bromophenyl)-6-(2-(diethylamino)ethylthio)pyridine-3,5-dicarbonitrile (10).**  $^1H$  NMR ( $CD_3OD/CD_3CO_2D$ )  $\delta$  7.74 (d,  $J = 8.8$  Hz, 2H), 7.44 (d,  $J = 8.4$  Hz, 2H), 3.60 (m, 2H), 3.48 (m, 2H), 3.34 (q,  $J = 7.2$  Hz, 4H), 1.35 (t,  $J = 7.2$  Hz, 6H); LCMS (ESI)  $m/z$  432 ( $MH^+$ ); HRMS  $m/z$  calculated for  $C_{19}H_{21}N_5SBr$  ( $MH^+$ ) 430.0701, found 430.0702; purity method A, 97%, method B, 95%.

**2-Amino-4-(3-bromophenyl)-6-(2-(diethylamino)ethylthio)pyridine-3,5-dicarbonitrile (11).**  $^1H$  NMR ( $CD_3OD/CD_3CO_2D$ )  $\delta$  7.75 (td,  $J = 2.0$  Hz, 4.8 Hz, 1H), 7.69 (d,  $J = 2.8$  Hz, 1H), 7.49 (d,  $J = 5.2$  Hz, 2H), 3.60 (m, 2H), 3.48 (m, 2H), 3.34 (q,  $J = 7.2$  Hz, 4H), 1.35 (t,  $J = 7.2$  Hz, 6H); LCMS (ESI)  $m/z$  432 ( $MH^+$ ); HRMS  $m/z$  calculated for  $C_{19}H_{21}N_5SBr$  ( $MH^+$ ) 430.0701, found 430.0697; purity method A, 97%, method B, 95%.

**2-(2-(Diethylamino)ethylthio)-6-amino-4-(3,5-dichlorophenyl)pyridine-3,5-dicarbonitrile (12).**  $^1H$  NMR ( $CD_3OD/CD_3CO_2D$ )  $\delta$  7.69 (t,  $J = 2.0$  Hz, 1H), 7.52 (d,  $J = 2.0$  Hz, 2H), 3.60 (m, 2H), 3.48 (m, 2H), 3.34 (q,  $J = 7.2$  Hz, 4H), 1.35 (t,  $J = 7.2$  Hz, 6H); LCMS (ESI)  $m/z$  421 ( $MH^+$ ); HRMS  $m/z$  calculated for  $C_{19}H_{20}N_5Cl_2S$  ( $MH^+$ ) 420.0816, found 420.0808; purity method A, 95%, method B, 95%.

**2-(2-(Diethylamino)ethylthio)-6-amino-4-(2,3-dichlorophenyl)pyridine-3,5-dicarbonitrile (13).**  $^1H$  NMR ( $CD_3OD/CD_3CO_2D$ )  $\delta$  7.76 (dd,  $J = 1.6, 8.0$  Hz, 1H), 7.51 (t,  $J = 8.0$  Hz, 1H), 7.36 (dd,  $J = 1.2, 7.6$  Hz, 1H), 3.60 (m, 2H), 3.48 (m, 2H), 3.34 (q,  $J = 7.2$  Hz, 4H), 1.35 (t,  $J = 7.2$  Hz, 6H); LCMS (ESI)  $m/z$  421 ( $MH^+$ ); HRMS  $m/z$  calculated for  $C_{19}H_{20}N_5Cl_2S$  ( $MH^+$ ) 420.0816, found 420.0807; purity method A, 93%, method B, 95%.

**2-(2-(Diethylamino)ethylthio)-6-amino-4-(3,4-dichlorophenyl)pyridine-3,5-dicarbonitrile (14).**  $^1H$  NMR ( $CD_3OD/CD_3CO_2D$ )  $\delta$  7.74 (d,  $J = 6.0$  Hz, 1H), 7.73 (s, 1H), 7.45 (dd,  $J = 2.4, 8.4$  Hz, 1H), 3.60 (m, 2H), 3.48 (m, 2H), 3.34 (q,  $J = 7.2$  Hz, 4H), 1.35 (t,  $J = 7.2$  Hz, 6H); LCMS (ESI)  $m/z$  421 ( $MH^+$ ); HRMS  $m/z$  calculated for  $C_{19}H_{20}N_5Cl_2S$  ( $MH^+$ ) 420.0816, found 420.0809; purity method A, 88%, method B, 100%.

**2-(6-Amino-3,5-dicyano-4-(furan-2-yl)pyridine-2-ylthio)acetamide (15).**  $^1H$  NMR ( $DMSO-d_6$ )  $\delta$  8.01 (s, 1H), 7.48 (bs, 2H), 7.39 (d,  $J = 3.2$  Hz, 1H), 7.23 (bs, 2H), 6.83 (s, 1H), 3.85 (s, 2H); LCMS (ESI)  $m/z$  300 ( $MH^+$ ); HRMS  $m/z$  calculated for  $C_{13}H_9N_5O_2NaSS$  ( $MNa^+$ ) 322.0375, found 322.0379; purity method A, 94%, method B, 100%.

**2-Amino-6-(3-aminopropylsulfanyl)-4-furan-2-ylpyridine-3,5-dicarbonitrile (16).**  $^1H$  NMR ( $CD_3OD/CD_3CO_2D$ )  $\delta$  7.86 (d,  $J = 1.2$  Hz, 1H), 7.47 (d,  $J = 3.2$  Hz, 1H), 6.74 (dd,  $J = 1.6, 3.6$  Hz, 1H), 3.34 (t,  $J = 7.2$  Hz, 2H), 3.07 (t,  $J = 7.6$  Hz, 2H), 2.09 (quintet,  $J = 7.6$  Hz, 2H);  $^{13}C$  NMR ( $DMSO-d_6$ ) 167.8, 160.1, 146.4, 145.1, 143.7, 116.2, 115.8, 115.7, 112.8, 89.7, 81.3, 31.6, 31.5, 27.3; LCMS (ESI)  $m/z$  300 ( $MH^+$ ); HRMS  $m/z$  calculated for  $C_{14}H_{13}N_5CONaS$  ( $MNa^+$ ) 322.0739, found 322.0733; purity method A, 69%, method B, 70%.

**2-(2-(Dimethylamino)ethylthio)-6-amino-4-(furan-2-yl)pyridine-3,5-dicarbonitrile (17).**  $^1H$  NMR ( $CD_3OD/CD_3CO_2D$ )  $\delta$  7.88 (d,  $J = 1.6$  Hz, 1H), 7.51 (d,  $J = 3.6$  Hz, 1H), 6.75 (dd,  $J = 1.6, 3.6$  Hz, 1H), 3.61 (m, 2H), 3.51 (m, 2H), 2.98 (s, 6H); LCMS (ESI)  $m/z$  314 ( $MH^+$ ); HRMS  $m/z$  calculated for  $C_{15}H_{15}N_5ONaS$  ( $MNa^+$ ) 336.0895, found 336.0901; purity method A, 97%, method B, 95%.

**2-(3-(Dimethylamino)propylthio)-6-amino-4-(furan-2-yl)pyridine-3,5-dicarbonitrile (18).**  $^1H$  NMR ( $DMSO-d_6$ )  $\delta$  8.10 (d,  $J = 1.6$  Hz, 1H), 7.39 (d,  $J = 3.6$  Hz, 1H), 6.84 (dd,  $J = 2.0, 3.6$  Hz, 1H), 3.22 (t,  $J = 6.8$  Hz, 2H), 3.14 (m, 2H), 3.09 (m, 2H), 2.76 (s, 6H); LCMS (ESI)  $m/z$  328 ( $MH^+$ ); HRMS  $m/z$  calculated for  $C_{16}H_{17}N_5ONaS$  ( $MNa^+$ ) 350.1052, found 350.1045; purity method A, 90%, method B, 100%.

**2-Amino-6-(2-diethylaminoethylsulfanyl)-4-furan-2-ylpyridine-3,5-dicarbonitrile (19).**  $^1H$  NMR ( $CD_3OD/CD_3CO_2D$ )  $\delta$  7.88 (d,  $J = 1.2$  Hz, 1H), 7.51 (d,  $J = 3.6$  Hz, 1H), 6.75 (dd,  $J = 1.6, 3.6$

Hz, 1H), 3.60 (m, 2H), 3.48 (m, 2H), 3.34 (q,  $J = 7.2$  Hz, 4H), 1.35 (t,  $J = 7.2$  Hz, 6H); LCMS (ESI)  $m/z$  342 (MH<sup>+</sup>); HRMS  $m/z$  calculated for C<sub>17</sub>H<sub>20</sub>N<sub>5</sub>O<sub>5</sub> (MH<sup>+</sup>) 342.1389, found 342.1375; purity method A, 99%, method B, 100%.

**2-Amino-6-(2-(diisopropylamino)ethylthio)-4-furan-2-ylpyridine-3,5-dicarbonitrile (20).** <sup>1</sup>H NMR (CD<sub>3</sub>OD/CD<sub>3</sub>CO<sub>2</sub>D)  $\delta$  7.88 (d,  $J = 1.2$  Hz, 1H), 7.51 (d,  $J = 3.6$  Hz, 1H), 6.75 (dd,  $J = 2.0$ , 3.6 Hz, 1H), 3.83 (quintet,  $J = 6.8$  Hz, 2H), 3.61 (m, 2H), 3.44 (m, 2H), 1.42 (d,  $J = 6.8$  Hz, 12H); LCMS (ESI)  $m/z$  370 (MH<sup>+</sup>); HRMS  $m/z$  calculated for C<sub>19</sub>H<sub>24</sub>N<sub>5</sub>O<sub>5</sub> (MH<sup>+</sup>) 370.1702, found 370.1701; purity method A, 95%, method B, 100%.

**2-(2-(Pyrrolidin-1-yl)ethylthio)-6-amino-4-(furan-2-yl)pyridine-3,5-dicarbonitrile (21).** <sup>1</sup>H NMR (CD<sub>3</sub>OD/CD<sub>3</sub>CO<sub>2</sub>D)  $\delta$  7.88 (s, 1H), 7.50 (d,  $J = 3.6$  Hz, 1H), 6.75 (dd,  $J = 1.6$ , 3.6 Hz, 1H), 3.58 (m, 6H), 3.48 (m, 2H), 2.12 (m, 4H); LCMS (ESI)  $m/z$  340 (MH<sup>+</sup>); HRMS  $m/z$  calculated for C<sub>17</sub>H<sub>18</sub>N<sub>5</sub>O<sub>5</sub> (MH<sup>+</sup>) 340.1232, found 340.1244; purity method A, 97%, method B, 100%.

**2-(2-(Piperidin-1-yl)ethylthio)-6-amino-4-(furan-2-yl)pyridine-3,5-dicarbonitrile (22).** <sup>1</sup>H NMR (CD<sub>3</sub>OD/CD<sub>3</sub>CO<sub>2</sub>D)  $\delta$  7.88 (d,  $J = 2.0$  Hz, 1H), 7.50 (d,  $J = 3.6$  Hz, 1H), 6.75 (dd,  $J = 1.6$ , 3.6 Hz, 1H), 3.65 (m, 2H), 3.59 (m, 2H), 3.45 (m, 2H), 3.04 (m, 2H), 1.95 (m, 2H), 1.83 (m, 3H), 1.55 (m, 1H); LCMS (ESI)  $m/z$  354 (MH<sup>+</sup>); HRMS  $m/z$  calculated for C<sub>18</sub>H<sub>20</sub>N<sub>5</sub>O<sub>5</sub> (MH<sup>+</sup>) 354.1389, found 354.1381; purity method A, 95%, method B, 100%.

**2-(3-(Piperidin-1-yl)propylthio)-6-amino-4-(furan-2-yl)pyridine-3,5-dicarbonitrile (23).** <sup>1</sup>H NMR (DMSO-*d*<sub>6</sub>)  $\delta$  8.10 (d,  $J = 1.2$  Hz, 1H), 7.39 (d,  $J = 3.6$  Hz, 1H), 6.83 (dd,  $J = 1.6$ , 3.6 Hz, 1H), 3.43 (m, 2H), 3.23 (t,  $J = 7.2$  Hz, 2H), 3.14 (m, 2H), 2.85 (m, 2H), 2.04 (m, 2H), 1.80 (m, 2H), 1.62 (m, 3H), 1.35 (m, 1H); LCMS (ESI)  $m/z$  368 (MH<sup>+</sup>); HRMS  $m/z$  calculated for C<sub>19</sub>H<sub>22</sub>N<sub>5</sub>O<sub>5</sub> (MH<sup>+</sup>) 368.1545, found 368.1537; purity method A, 93%, method B, 100%.

**2-(2-Morpholinoethylthio)-6-amino-4-(furan-2-yl)pyridine-3,5-dicarbonitrile (24).** <sup>1</sup>H NMR (CD<sub>3</sub>OD/CD<sub>3</sub>CO<sub>2</sub>D)  $\delta$  7.88 (d,  $J = 1.2$  Hz, 1H), 7.50 (d,  $J = 3.2$  Hz, 1H), 6.75 (dd,  $J = 2.0$ , 3.6 Hz, 1H), 3.92 (m, 4H), 3.59 (m, 2H), 3.46 (m, 2H), 3.35 (m, 4H); LCMS (ESI)  $m/z$  356 (MH<sup>+</sup>); HRMS  $m/z$  calculated for C<sub>17</sub>H<sub>17</sub>N<sub>5</sub>O<sub>2</sub>-NaS (MNa<sup>+</sup>) 378.1001, found 378.1002; purity method A, 87%, method B, 100%.

**2-(2-(Dibutylamino)ethylthio)-6-amino-4-(furan-2-yl)pyridine-3,5-dicarbonitrile (25).** <sup>1</sup>H NMR (CD<sub>3</sub>OD/CD<sub>3</sub>CO<sub>2</sub>D)  $\delta$  7.88 (s, 1H), 7.50 (d,  $J = 3.6$  Hz, 1H), 6.75 (dd,  $J = 1.6$ , 3.6 Hz, 1H), 3.61 (m, 2H), 3.52 (m, 2H), 3.25 (m, 4H), 1.72 (m, 4H), 1.45 (m, 4H), 1.01 (t,  $J = 7.2$  Hz, 6H); LCMS (ESI)  $m/z$  398 (MH<sup>+</sup>); HRMS  $m/z$  calculated for C<sub>21</sub>H<sub>28</sub>N<sub>5</sub>O<sub>5</sub> (MH<sup>+</sup>) 398.2015, found 398.2011; purity method A, 95%, method B, 100%.

**2-(2-(*N*-Benzyl-*N*-methylamino)ethylthio)-6-amino-4-(furan-2-yl)pyridine-3,5-dicarbonitrile (26).** <sup>1</sup>H NMR (CD<sub>3</sub>OD/CD<sub>3</sub>CO<sub>2</sub>D)  $\delta$  7.89 (d,  $J = 1.6$  Hz, 1H), 7.50 (d,  $J = 3.6$  Hz, 1H), 7.46 (m, 5H), 6.76 (dd,  $J = 1.6$ , 3.6 Hz, 1H), 4.41 (s, 2H), 3.60 (m, 2H), 3.51 (m, 2H), 2.97 (s, 3H); LCMS (ESI)  $m/z$  390 (MH<sup>+</sup>); HRMS  $m/z$  calculated for C<sub>21</sub>H<sub>20</sub>N<sub>5</sub>O<sub>5</sub> (MH<sup>+</sup>) 390.1389, found 390.1385; purity method A, 89%, method B, 100%.

**General Procedure B. Synthesis of Thienopyridine Compounds.** Thienopyridines **6** were prepared according to the procedure of Dyachenko et al. Briefly, pyridine compounds **5** were treated with 10% aqueous KOH (1 equiv) in DMF (0.4 mL) for 5 h at the room temperature. The product was precipitated by the addition of H<sub>2</sub>O (0.4 mL) and collected by filtration, washed with ice-cold H<sub>2</sub>O (5 mL), ice-cold ethanol (5 mL), and hexanes (5 mL) and dried under high vacuum. Compounds were obtained in 60–80% yields.

**3,6-Diamino-4-furan-2-yl-2-(2-nitrobenzoyl)thieno[2,3-*b*]pyridine-5-carbonitrile (28).** <sup>1</sup>H NMR (DMSO-*d*<sub>6</sub>)  $\delta$  8.17 (d,  $J = 8.0$  Hz, 1H), 8.12 (bs, 1H), 7.90 (t,  $J = 7.2$  Hz, 1H), 7.78 (d,  $J = 8.0$  Hz, 1H), 7.75 (bs, 1H), 7.70 (d,  $J = 7.2$  Hz, 1H), 7.22 (bs, 1H), 6.88 (dd,  $J = 1.6$ , 3.6 Hz, 1H); LCMS (ESI)  $m/z$  406 (MH<sup>+</sup>); HRMS  $m/z$  calculated for C<sub>19</sub>H<sub>12</sub>N<sub>5</sub>O<sub>4</sub>S (MH<sup>+</sup>) 406.0610, found 406.0602; purity method A, 69%, method B, 95%.

**3,6-Diamino-4-furan-2-yl-2-(2,3-dihydrobenzo[*b*]1,4)dioxan-2-yl)thieno[2,3-*b*]pyridine-5-carbonitrile (29).** <sup>1</sup>H NMR (DMSO-*d*<sub>6</sub>)  $\delta$  8.10 (s, 1H), 7.66 (bs, 1H), 7.24 (d,  $J = 8.4$  Hz, 1H), 7.19

(bs, 1H), 7.18 (d,  $J = 3.2$  Hz, 1H), 6.96 (d,  $J = 8.4$  Hz, 1H), 6.86 (dd,  $J = 1.6$ , 3.6 Hz, 1H), 4.30 (d,  $J = 4.8$  Hz, 4H); LCMS (ESI)  $m/z$  419 (MH<sup>+</sup>); HRMS  $m/z$  calculated for C<sub>21</sub>H<sub>14</sub>N<sub>4</sub>O<sub>4</sub>NaS (MNa<sup>+</sup>) 441.0633, found 441.0631; purity method A, 74%, method B, 95%.

**Duplex Cellular Toxicity and Antiprion Assay.** ScN2a cells were maintained in filter-sterilized (0.2  $\mu$ m) MEM, supplemented with FBS and GlutaMax. On day 1, media was aspirated from a confluent 100 mm plate of ScN2a cells and cells were detached by addition of 0.05% trypsin–EDTA (1 mL). MEM media was added (approximately 10 mL), and the cell concentration was determined using Packed Cell Volume tubes (TPP). The ScN2a cell concentration was adjusted to  $4 \times 10^5$  cells mL<sup>-1</sup> with MEM media. A 96-well, tissue-culture-treated, clear-bottom, black plate (Greiner Bio-One) wetted with MEM media (90  $\mu$ L) was incubated at 37 °C prior to use. To this plate, 100  $\mu$ L of the ScN2a cell suspension was transferred, and the cells were allowed to settle for 2 h prior to addition of the test compound. Compound libraries were prepared in 100% DMSO at the required concentrations in a 96-well format and then diluted <sup>1</sup>/<sub>20</sub> with sterile PBS prior to use. Compounds (10  $\mu$ L) were transferred to the 96-well cell culture plate, and the plates were incubated at 37 °C. Final DMSO concentrations did not exceed 0.25% (v/v). Media were aspirated on day 5, and cells were washed twice with PBS (200  $\mu$ L). Calcein-AM (100  $\mu$ L, 2.5  $\mu$ g mL<sup>-1</sup> solution in PBS) was added, and the plates were incubated at 37 °C for 25 min. Fluorescent emission intensity was quantified using a fluorescence plate reader, ex/em = 492 nm/525 nm.

The calcein-AM solution was aspirated, 50  $\mu$ L of lysis buffer (10 mM Tris-HCl, pH 8.0; 150 mM NaCl; 0.5% sodium deoxycholate; 0.5% Nonidet P-40) was added, and then plates were shaken for 5 min at room temperature. Benzoylase nuclease (25  $\mu$ L, 7.5 U/mL in 50 mM Tris-HCl, pH 8.0; 20 mM NaCl; 2 mM MgCl<sub>2</sub>) was added, and plates were incubated at 37 °C for 15 min or until the DNA pellet was no longer visible. Proteinase K (25  $\mu$ L, 25  $\mu$ g mL<sup>-1</sup> solution in lysis buffer) was added, and the plates were incubated at 37 °C for 1 h. Proteolysis was inhibited by the addition of PMSF (10  $\mu$ L, 20 mM solution in ethanol), with a 10 min incubation at room temperature. PK-digested PrP<sup>Sc</sup> was precipitated by the addition of PTA (110  $\mu$ L, 7.5% solution in 64.75 mM MgCl<sub>2</sub>, pH 7.4). Plates were incubated overnight at 37 °C and then centrifuged at 2200 rpm for 60 min using a Beckman-Coulter GS-6R centrifuge. The supernatant was aspirated. The PTA-precipitated protein pellet was denatured with 6 M guanidine thiocyanate (55  $\mu$ L) in coating buffer (55  $\mu$ L, 0.1 M sodium bicarbonate, pH 8.6) for 5 min at room temperature with shaking. The suspension (100  $\mu$ L) was transferred to Immulon II ELISA plates (Fisher Scientific), sealed, and incubated overnight at 4 °C. ELISA plates were washed twice with TBST (20 mM Tris-HCl, 137 mM NaCl, 0.05% Tween-20, pH 7.5), blocked with 200  $\mu$ L of 3% BSA as a solution in TBS (20 mM Tris-HCl, 137 mM NaCl, pH 7.5), sealed, and incubated at 37 °C. After 1 h, the ELISA plates were washed twice with TBST and incubated with 100  $\mu$ L of anti-PrP antibody D18 (1  $\mu$ g mL<sup>-1</sup>) as a solution in 1% BSA/TBS. ELISA plates were sealed and incubated at 37 °C for 2 h, then washed seven times with TBST. Goat antihuman IgG Fab AP conjugate (100  $\mu$ L) diluted 1:2500 with 1% BSA/TBS was added to the plates, sealed, and incubated at 37 °C for 1 h. Plates were washed seven times with TBST. Plates were developed with *p*-nitrophenyl phosphate (100  $\mu$ L, 1 mg mL<sup>-1</sup>) as a solution in alkaline phosphatase buffer (1 M diethanolamine, 0.5 mM MgCl<sub>2</sub>·6H<sub>2</sub>O, pH 9.8). Absorbance at 405 nm was measured using a microplate reader. Dose-response curves and EC<sub>50</sub> values were computed using SigmaPlot.

**Duplex Solubility and PAMPA Assay.** Compound stocks at 10 mM were serially diluted over a concentration range of 500–3.13  $\mu$ M in DMSO (final volume 200  $\mu$ L) in a UV-compatible, 96-well plate (Greiner Bio-One), in triplicate. Absorbance at 320 nm was quantified using a SpectraMax microplate reader and a standard curve was derived such that  $r^2 > 0.85$ . Standard curves for control compounds were determined at an appropriate absorption maxima. A membrane-embedded solubility plate (Millipore) was wetted with previously filtered donor buffer (275  $\mu$ L, 50 mM

potassium phosphate (monobasic), pH 6.5). To the solubility plate, 15  $\mu\text{L}$  of test compound at 10 mM in DMSO was added, and the plate was shaken at room temperature for 90 min. Vacuum was applied to the underside of the membrane plate using a vacuum manifold (Millipore), and the filtrate was collected in a 96-well receiver plate. Filtrate (200  $\mu\text{L}$ ) was transferred to a UV-compatible, 96-well plate (Greiner Bio-One). Absorbance at 320 nm was measured  $\{A_{\text{max}}(\text{filtrate})\}$ , and the concentration was derived from the linear slope of the standard curve. The filtrate was retained for the secondary permeability screen. Compound solubility was categorized as follows: 0  $\mu\text{M}$  < “poor” < 200  $\mu\text{M}$ ; 200  $\mu\text{M}$  < “medium” < 400  $\mu\text{M}$ ; “excellent” > 400  $\mu\text{M}$ .

For the permeability screen, a PAMPA sandwich was prepared by transferring filtered (0.2 mm) acceptor buffer (300  $\mu\text{L}$ , 50 mM potassium phosphate (monobasic), 2% DMSO, pH 7.4) to a Teflon acceptor plate (Millipore). A PAMPA donor plate (Millipore) was coated with 4  $\mu\text{L}$  of DOPC lipid, as a solution in dodecane, with 1% BHT additive (Avanti Polar Lipids). Filtrate from the solubility assay (150  $\mu\text{L}$ ) was carefully added to the donor plate, and the PAMPA sandwich was assembled. The sandwich was incubated at room temperature in the dark for 15 h and then disassembled. Acceptor buffer (200  $\mu\text{L}$ ) was transferred from the Teflon acceptor block to a UV-compatible, 96-well plate (Greiner Bio-One), and absorbance was measured at 320 nm  $\{A_{\text{max}}(\text{acceptor})\}$ . Permeability ( $\log P_e$ ) was calculated on the basis of the formula of Wohnsland et al.:

$$C = \frac{V_D V_A}{(\text{area})(\text{time})}$$

$$\log P_e = \log \left\{ C \left[ -\ln \left( 1 - \frac{A_{\text{max}}(\text{acceptor})}{A_{\text{max}}(\text{filtrate})} \right) \right] \right\}$$

for which  $V_D = 0.15 \text{ cm}^3$  (150  $\mu\text{L}$ ),  $V_A = 0.30 \text{ cm}^3$  (300  $\mu\text{L}$ ), area = 0.048  $\text{cm}^2$ , time = 54 000 s (15 h).

**Acknowledgment.** This work was supported by the National Institutes of Health (Grants AG02132, AG10770, and AG021601) and by a gift from the G. Harold and Leila Y. Mathers Charitable Foundation. The authors thank Hang Nguyen, Cedric Covaerts, and Jay Choi (UCSF) for assistance in preparation of this manuscript. B.C.H.M., S.B.P. and G.L. have financial interest in InPro Biotechnology, Inc. (California).

**Supporting Information Available:** NMR, MS, and and bioactivity data. This material is available free of charge via the Internet at <http://pubs.acs.org>.

## References

- Prusiner, S. B. Prions. *Proc. Natl. Acad. Sci. U.S.A.* **1998**, *95* (23), 13363–13383.
- DeArmond, S. J.; Prusiner, S. B. Transgenetics and neuropathology of prion diseases. *Curr. Top. Microbiol. Immunol.* **1996**, *207*, 125–146.
- Telling, G. C.; Scott, M.; Mastrianni, J.; Gabizon, R.; Torchia, M.; Cohen, F. E.; DeArmond, S. J.; Prusiner, S. B. Prion propagation in mice expressing human and chimeric PrP transgenes implicates the interaction of cellular PrP with another protein. *Cell* **1995**, *83* (1), 79–90.
- Kaneko, K.; Zulianello, L.; Scott, M.; Cooper, C. M.; Wallace, A. C.; James, T. L.; Cohen, F. E.; Prusiner, S. B. Evidence for protein X binding to a discontinuous epitope on the cellular prion protein during scrapie prion propagation. *Proc. Natl. Acad. Sci. U.S.A.* **1997**, *94* (19), 10069–10074.
- Kitamoto, T.; Tateishi, J. Human prion diseases with variant prion protein. *Philos. Trans. R. Soc. London, Ser. B* **1994**, *343* (1306), 391–398.
- Westaway, D.; Zuliani, V.; Cooper, C. M.; Da Costa, M.; Neuman, S.; Jenny, A. L.; Detwiler, L.; Prusiner, S. B. Homozygosity for prion protein alleles encoding glutamine-171 renders sheep susceptible to natural scrapie. *Genes Dev.* **1994**, *8* (8), 959–969.
- Perrier, V.; Kaneko, K.; Safar, J.; Vergara, J.; Tremblay, P.; DeArmond, S. J.; Cohen, F. E.; Prusiner, S. B.; Wallace, A. C. Dominant-negative inhibition of prion replication in transgenic mice. *Proc. Natl. Acad. Sci. U.S.A.* **2002**, *99* (20), 13079–13084.
- Perrier, V.; Wallace, A. C.; Kaneko, K.; Safar, J.; Prusiner, S. B.; Cohen, F. E. Mimicking dominant negative inhibition of prion replication through structure-based drug design. *Proc. Natl. Acad. Sci. U.S.A.* **2000**, *97* (11), 6073–6078.
- Gazit, A.; Osherov, N.; Posner, I.; Yaish, P.; Poradosu, E.; Gilon, C.; Levitzki, A. Tyrphostins. 2. Heterocyclic and alpha-substituted benzylidenemalononitrile tyrphostins as potent inhibitors of EGF receptor and ErbB2/neu tyrosine kinases. *J. Med. Chem.* **1991**, *34* (6), 1896–1907.
- Yvachenko, V. D.; Litvinov, V. P. Synthesis and recyclization of 4-aryl-2,6-diamino-3,5-dicyano-4H-thiopyrans. *Russ. J. Org. Chem.* **1998**, *34* (4), 557–563.
- Kambe, S.; Saito, K.; Sakurai, A.; Midorikawa, H. Synthetic studies using alpha,beta-unsaturated nitriles: facile synthesis of pyridine derivatives. *Synthesis* **1981**, 531–532.
- Butler, D. A.; Scott, M. R.; Bockman, J. M.; Borchelt, D. R.; Taraboulos, A.; Hsiao, K. K.; Kingsbury, D. T.; Prusiner, S. B. Scrapie-infected murine neuroblastoma cells produce protease-resistant prion proteins. *J. Virol.* **1988**, *62* (5), 1558–1564.
- Oesch, B.; Westaway, D.; Walchli, M.; McKinley, M. P.; Kent, S. B.; Aebersold, R.; Barry, R. A.; Tempst, P.; Teplow, D. B.; Hood, L. E.; Prusiner, S. B.; Weissmann, C. A cellular gene encodes scrapie PrP 27–30 protein. *Cell* **1985**, *40* (4), 735–746.
- Lee, I. S.; Long, J. R.; Prusiner, S. B.; Safar, J. G. Selective precipitation of prions by polyoxometalate complexes. *J. Am. Chem. Soc.* **2005**, *127* (40), 13802–13803.
- Williamson, R. A.; Peretz, D.; Pinilla, C.; Ball, H.; Bastidas, R. B.; Rozenshteyn, R.; Houghten, R. A.; Prusiner, S. B.; Burton, D. R. Mapping the prion protein using recombinant antibodies. *J. Virol.* **1998**, *72* (11), 9413–9418.
- Korth, C.; May, B. C.; Cohen, F. E.; Prusiner, S. B. Acridine and phenothiazine derivatives as pharmacotherapeutics for prion disease. *Proc. Natl. Acad. Sci. U.S.A.* **2001**, *98* (17), 9836–9841.
- Wexler, D. S.; Gao, L.; Anderson, F.; Ow, A.; Nadasdi, L.; McAlorum, A.; Urfer, R.; Huang, S. G. Linking solubility and permeability assays for maximum throughput and reproducibility. *J. Biomol. Screening* **2005**, *10* (4), 383–390.
- Kansy, M.; Senner, F.; Gubernator, K. Physicochemical high throughput screening: parallel artificial membrane permeation assay in the description of passive absorption processes. *J. Med. Chem.* **1998**, *41* (7), 1007–1010.
- Wohnsland, F.; Faller, B. High-throughput permeability pH profile and high-throughput alkane/water log P with artificial membranes. *J. Med. Chem.* **2001**, *44* (6), 923–930.
- Aires-de-Sousa, J.; Gasteiger, J.; Gutman, I.; Vidovic, D. Chirality codes and molecular structure. *J. Chem. Inf. Comput. Sci.* **2004**, *44* (3), 831–836.
- Bostrom, J.; Greenwood, J. R.; Gottfries, J. Assessing the performance of OMEGA with respect to retrieving bioactive conformations. *J. Mol. Graphics Modell.* **2003**, *21* (5), 449–462.
- Wolber, G. Fast neutron beams for boron neutron capture therapy? *Z. Med. Phys.* **2004**, *14* (1), 55–63.
- Rudyk, H.; Vasiljevic, S.; Hennion, R. M.; Birkett, C. R.; Hope, J.; Gilbert, I. H. Screening Congo Red and its analogues for their ability to prevent the formation of PrP-res in scrapie-infected cells. *J. Gen. Virol.* **2000**, *81* (4), 1155–1164.
- Kocisko, D. A.; Baron, G. S.; Rubenstein, R.; Chen, J.; Kuizon, S.; Caughey, B. New inhibitors of scrapie-associated prion protein formation in a library of 2000 drugs and natural products. *J. Virol.* **2003**, *77* (19), 10288–10294.
- May, B. C.; Witkop, J.; Sherrill, J.; Anderson, M. O.; Madrid, P. B.; Zorn, J. A.; Prusiner, S. B.; Cohen, F. E.; Guy, R. K. Structure–activity relationship study of 9-aminoacridine compounds in scrapie-infected neuroblastoma cells. *Bioorg. Med. Chem. Lett.* **2006**, *16* (18), 4913–4916.
- Lichtenfels, R.; Biddison, W. E.; Schulz, H.; Vogt, A. B.; Martin, R. CARE-LASS (calcein-release-assay), an improved fluorescence-based test system to measure cytotoxic T lymphocyte activity. *J. Immunol. Methods* **1994**, *172* (2), 227–239.
- Zhang, J. H.; Chung, T. D.; Oldenburg, K. R. A simple statistical parameter for use in evaluation and validation of high throughput screening assays. *J. Biomol. Screening* **1999**, *4* (2), 67–73.
- Lipinski, C. A.; Lombardo, F.; Dominy, B. W.; Feeney, P. J. Experimental and computational approaches to estimate solubility and permeability in drug discovery and development settings. *Adv. Drug Delivery Rev.* **2001**, *46* (1–3), 3–26.



- (29) Reddy, T. R.; Mutter, R.; Heal, W.; Guo, K.; Gillet, V. J.; Pratt, S.; Chen, B. Library design, synthesis, and screening: pyridine dicarbonitriles as potential prion disease therapeutics. *J. Med. Chem.* **2006**, *49* (2), 607–615.
- (30) Beukers, M. W.; Chang, L. C.; von Frijtag Drabbe Kunzel, J. K.; Mulder-Krieger, T.; Spanjersberg, R. F.; Brussee, J.; IJzerman, A. P. New, non-adenosine, high-potency agonists for the human adenosine A<sub>2B</sub> receptor with an improved selectivity profile compared to the reference agonist *N*-ethylcarboxamidoadenosine. *J. Med. Chem.* **2004**, *47* (15), 3707–3709.
- (31) Chang, L. C.; von Frijtag Drabbe Kunzel, J. K.; Mulder-Krieger, T.; Spanjersberg, R. F.; Roerink, S. F.; van den Hout, G.; Beukers, M. W.; Brussee, J.; IJzerman, A. P. A series of ligands displaying a remarkable agonistic–antagonistic profile at the adenosine A1 receptor. *J. Med. Chem.* **2005**, *48* (6), 2045–2053.
- (32) Haleen, S. J.; Steffen, R. P.; Hamilton, H. W. PD 116,948, a highly selective A1 adenosine receptor antagonist. *Life Sci.* **1987**, *40* (6), 555–561.
- (33) Gallo-Rodriguez, C.; Ji, X. D.; Melman, N.; Siegman, B. D.; Sanders, L. H.; Orlina, J.; Fischer, B.; Pu, Q.; Olah, M. E.; van Galen, P. J.; et al. Structure–activity relationships of N6-benzyladenosine-5'-uronamides as A3-selective adenosine agonists. *J. Med. Chem.* **1994**, *37* (5), 636–646.
- (34) Townsend-Nicholson, A.; Schofield, P. R. A threonine residue in the seventh transmembrane domain of the human A1 adenosine receptor mediates specific agonist binding. *J. Biol. Chem.* **1994**, *269* (4), 2373–2376.
- (35) Govaerts, C.; Wille, H.; Prusiner, S. B.; Cohen, F. E. Evidence for assembly of prions with left-handed beta-helices into trimers. *Proc. Natl. Acad. Sci. U.S.A.* **2004**, *101* (22), 8342–8347.

JM061045Z